CrossMark

CAMBRIDGE
UNIVERSITY PRESS

RESEARCH ARTICLE

Searching for biosignatures by their rotational spectrum: global fit and methyl group internal rotation features of dimethylsulphoxide up to 116 GHz

Assimo Maris[1,2] (iD), Laura B. Favero[3], Wentao Song[1], Dingding Lv[1], Luca Evangelisti[2,4] (iD) and Sonia Melandri[1,2] (iD)

[1]Department of Chemistry 'Giacomo Ciamician', Alma Mater Studiorum-University of Bologna, Via Francesco Selmi 2, I-40126 Bologna, Italy
[2]Interdepartmental Centre for Industrial Aerospace Research (CIRI Aerospace), Alma Mater Studiorum-University of Bologna, Via Baldassarre Canaccini 12, I-47121 Forlì, Italy
[3]Istituto per lo Studio dei Materiali Nanostrutturati, Sezione di Bologna, Consiglio Nazionale delle Ricerche (CNR), Via Gobetti 101, I-40129 Bologna, Italy
[4]Department of Chemistry 'Giacomo Ciamician', Alma Mater Studiorum-University of Bologna, Via S. Alberto 163, I-48123 Ravenna, Italy

Author for correspondence: Sonia Melandri, E-mail: sonia.melandri@unibo.it

Abstract

The identification and quantification of molecules in interstellar space and atmospheres of planets in the solar systems and in exoplanets rely on spectroscopic methods and laboratory work is essential to provide the community with the spectral features needed to analyse cosmological observations. Rotational spectroscopy in particular, with its intrinsic high resolution, allows the unambiguous identification of biomolecular building blocks and biosignature gases which can be correlated with the origin of life or the identification of habitable planets. We report the extension of the measured rotational transition frequencies of dimethylsulphoxide and its ^{34}S and ^{13}C isotopologues in the millimetre wave range (59.6–78.4 GHz) by use of an absorption spectrometer based on the supersonic expansion technique. Hyperfine patterns related to the methyl group internal rotation were analysed in the microwave range region (6–18 GHz) with a Pulsed Jet Fourier Transform spectrometer at extremely high resolution (2 kHz) and reliable predictions up to 116 GHz are provided. The focus on sulphur-bearing molecules is motivated by the fact that sulphur is largely involved in the intra- and inter-molecular hydrogen bonds in proteins and although it is the 10th most abundant element in the known Universe, understanding its chemistry is still a matter of debate. Moreover, sulphur-bearing molecules, in particular dimethylsulphoxide, have been indicated as possible biosignature gases to be monitored in the search of habitable exoplanets.

Contents

Introduction

The search for gaseous molecules in space is a guiding goal in the astrophysical community. The molecules searched for are of increasing complexity in the pursue of understanding the chemical steps that

lead to the development of complex molecules, biomolecular building blocks and ultimately life. Another goal is the search for molecules produced by living organisms, called biosignatures, and accumulated in the atmospheres of planets and exoplanets to assess their habitability.

As regards the detection of biosignatures, the early paradigm for exoplanet life detection is the argument that only life can maintain gases severely out of thermodynamic equilibrium in the atmosphere. In particular, the detection of oxygen (O_2) and methane (CH_4) (Lederberg, 1965; Lovelock, 1965) was suggested as the most robust atmospheric evidence of life on Earth.

In general, biosignature gases can be those created directly by metabolic redox reactions or they can be 'secondary' metabolism byproducts: gases produced by life but not as byproducts of their central chemical functions. Such gases are usually related to stress or signalling in living beings and although expected to be produced in small quantities, their specificity makes them valuable as possible biosignatures as their detection is not likely to be a false positive (Seager *et al.*, 2012). Some are also produced in sufficient amounts to affect atmospheric chemistry (such as isoprene or dimethyl sulphide) and they could possibly be detected remotely on planets and exoplanets. Examples include nitrous oxide (N_2O) (Des Marais *et al.*, 2002), dimethyldisulphide (CH_3SSCH_3) (Pilcher, 2003), methyl chloride (CH_3Cl) (Segura *et al.*, 2005) and dimethyl sulphide (CH_3SCH_3, DMS) and other sulphur gases (Domagal-Goldman *et al.*, 2011).

Recently, it has been pointed out that although atmospheric composition will be the primary observable that could imply the presence of life (Seager, 2013) the identification of a biosignature in a planet's atmosphere requires an understanding of the possible compositions of abiotic atmospheres (Shahar *et al.*, 2019).

This last factor is important as the atmosphere is tied to the dynamics of the planet and some secondary metabolism gases are produced by geological processes as well as biological ones.

As an example, we can consider a sulphur-containing molecule, namely dimethylsulphoxide (CH_3SOCH_3, DMSO, Fig. 1). DMSO is the product of oxidation of DMS, it can be directly produced by some microorganisms from DMS or it can be produced in the atmosphere through a non-biological chemical reaction which oxidizes DMS to DMSO, dimethyl sulphone ($CH_3SO_2CH_3$) and finally, methyl sulphate (CH_3SO_3H) (Seager *et al.*, 2012). In any case the detection and quantification of a molecule like DMSO would be important either as a biosignature itself or in the construction of appropriate models of chemical reactivity in the atmosphere of planets and exoplanets.

The most informative method to investigate the chemical composition of the atmospheres of planets and exoplanets is high-resolution spectroscopy, which for exoplanets must rely on remote-sensing techniques (Burrows, 2014). One of the possible approaches is via rotational spectroscopy in the microwave-to submillimetre range undertaken from the ground with radiotelescopes (see e.g. Greaves *et al.*, 2021). As regards the interstellar space and star-forming regions, the unequivocal identification of the molecules in astronomical surveys is based on their rotational laboratory spectra and more than 200 molecules have been identified in space (CDMS, 2001; Müller *et al.*, 2001, 2005). In addition to the characterization of the species, the features of molecular spectra also yield detailed physical information on the gas and its surroundings (Herbst and van Dishoeck, 2009).

Laboratory rotational spectroscopy data in the microwave, millimetre and submillimetre wavelengths are necessary to perform those searches and rotational spectroscopy performed in supersonic expansions has been proved to be particularly suitable to investigate complex spectra generated by molecules (Calabrese *et al.*, 2016) and weakly bound molecular complexes (Velino *et al.*, 2004; Favero *et al.*, 2010). Those experiments allow us to identify multiple conformers of a flexible molecule (Vigorito *et al.*, 2017a), different tautomers (Sanchez *et al.*, 2007; Melandri *et al.*, 2010) as well as and different isotopologues (Calabrese *et al.*, 2014). The study of the different isotopologues of a molecule is of importance for different reasons. From a structural point of view, the analysis of the changes in the rotational constants upon isotopic substitution allows the determination of the position of the substituted atoms without any *a priori* assumptions (Evangelisti *et al.*, 2015). If the collection of a complete
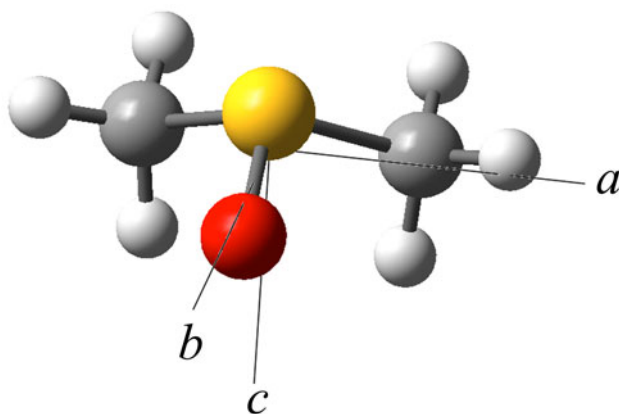
Fig. 1. *Sketch of the DMSO molecule and principal inertial axis.*

set of data including all the isotopes is not possible to achieve, a partial structure can be obtained by refining a structure obtained as a result of quantum chemical calculations to reproduce all experimental data (Uriarte *et al*., 2018). From an astrochemical point of view the detected abundance of different isotopologues of a molecular species can give additional information on reaction mechanisms of formation (Neill *et al*., 2011) or on the environment in which the molecule is found or formed (Imai *et al*., 2018).

We concentrate here on DMSO, which as stated above, can be considered an important secondary metabolic product or the product of an abiogenic mechanism occurring in the atmosphere or in geological processes. Also, DMSO is an important substance commonly used as a polar aprotic solvent, antifreeze fluid and cryo-protectant owing to its beneficial properties including low toxicity and environmental compatibility (Akkök *et al*., 2009). In this paper, we report our investigation on DMSO: the extension of the analysis of the rotational spectra of the parent species and that of the mono-substituted ^{13}C and ^{34}S isotopologues to the 59.6–78.4 GHz frequency range observed with a Free Jet Absorption Millimetre Wave (FJ-AMMW) spectrometer and the measurements of some transitions in the lower frequency region (6–18 GHz) with a high-resolution cavity-based Fourier transform microwave (FTMW) spectrometer. The extension of the measurement of the rotational spectrum to relatively high frequencies (>40 GHz) is very important, in particular for remote sensing using telescopes, since many of them, including ALMA, work in higher frequency regions. Even if the theoretical model used to analyse the spectrum in the low frequency region is correct, the uncertainties on the parameters reflect on the predictions thus precise experimental frequencies are essential for the identification of molecular transition in astronomical surveys or complex spectra containing the signals of many other molecules.

Experimental methods

Two different spectrometers working in the microwave and millimetre frequency regions have been utilized in this experiment. DMSO was acquired from Sigma-Aldrich (purity >99%) and used without further purification and argon or helium, purchased from SIAD (Società Italiana Acetilene e Derivati), were used as carrier gas.

The rotational spectrum of DMSO was recorded in the millimetre wave region (59.6–78.4 GHz) using a stark-modulated FJ-AMMW spectrometer with a resolution of about 300 kHz and estimated uncertainties for the frequency measurements of about 50 kHz. The main features of the spectrometer have been previously described (Calabrese *et al*., 2013, 2015; Vigorito *et al*., 2018). In this experiment the sample was maintained at room temperature and a stream of argon ($P_0 = 20$ kPa) was flowed over it

and the mixture was expanded to about $P_b = 0.5$ Pa through a 0.3 mm diameter pinhole nozzle. The rotational temperature of the molecules in the jet has been estimated to be 5–10 K from relative intensity measurements of rotational transitions at different rotational quantum numbers.

The measurement of the rotational spectrum in the 6–18 GHz region was carried out in a COBRA-type, cavity-based, pulsed supersonic-jet FTMW spectrometer (Balle and Flygare, 1981; Grabow *et al.*, 1996) previously described (Caminati *et al.*, 2016). The sample of DMSO was cooled to 273 K and helium was flowed over it at a stagnation pressure of about 3 bar resulting in a mixture of about 1%. The mixture was then expanded through a solenoid valve (General Valve, Series 9, nozzle diameter 0.5 mm) into a Fabry–Pérot cavity. During the expansion, the molecules can reach quite low-rotational temperatures (a few Kelvins) and the most stable forms can be trapped at their energy minimum when certain conditions are satisfied. To determine the position of the spectral lines, Fourier transformation of the time-domain signal perform 8k data points, recorded at a sampling interval of 100 ns.

Results and discussion

In terms of chemical structure, the rigid molecule of DMSO has idealized C_s symmetry and a trigonal pyramidal molecular geometry (Fig. 1). DMSO is characterized by two equivalent methyl rotors and a Cs frame, therefore, its molecular symmetry group is G_{18}^{WV} in Altmann's notation (Smeyers and Niño, 1987) and $C_3^- \times C_3^{v+}$ in Dreizler's approach (Dreizler, 1961). Due to the coupling of the methyl internal rotation to the overall rotation of the molecule, the rotational levels are split into a multiplet of four states labelled according to the irreducible representation in the above groups. Since, as Dreizler states, μ_a and μ_b transform as the AA_2 representation, in the vibronic ground state only four kinds of transitions are allowed: AA_1–AA_2, AE–AE, $(E_bA_1 + E_aA_1)$–$(E_bA_2 + E_aA_2)$ and $(E_aE + E_bE)$–$(E_aE + E_bE)$, with spin statistical weights 16, 8, 8 and 32, respectively. In the following, we will use a simplified notation, referring to the AA_1 and AA_2 states as AA, to $(E_bA_1 + E_aA_1)$ and $(E_bA_2 + E_aA_2)$ as EA and to $(E_aE + E_bE)$ and $(E_aE + E_bE)$ as EE. A good general graphical representation of the energy levels for a two tops system has been recently published (Dindić and Nguyen, 2021). Due to this splitting of the rotational levels, DMSO exhibits a spectral splitting because of hindered internal rotation of its methyl rotors that leads to a triplets AA, AE (or EA) and EE splitting pattern, where A and E are the methyl torsional state symmetry labels (see e.g. Vigorito *et al.*, 2017b).

The first rotational spectroscopy study on DMSO dates back to 1964 (Dreizler and Dendl, 1964) and several other studies followed focusing on the determination of the structure through the study of isotopologues (Feder *et al.*, 1969; Typke, 1978; Kretschmer, 1995) and the dynamic effects such as the centrifugal distortion and the methyl internal rotation (Dreizler and Dendl, 1965a, 1965b; Fliege *et al.*, 1983). The analysis of the high resolution rotational spectrum of the parent species is reported in Fliege *et al.* (1983) who explored the microwave spectrum of DMSO using a Fourier transform spectrometer from 8 to 18 GHz. They report the fit of the new measured lines together with the lines previously measured in the 6–40 GHz frequency range at a lower resolution. The observed transitions involve the dipole moment component along the *b* principal axis of rotation (μ_b-type) and the frequency values used are the weighted means of the internal rotation fine structure components. Also, seven other transitions involving the coupling of the radiation with the *c* principal axis (μ_c-type) were measured by radiofrequency-double resonance with pump frequency adjustment and methyl internal rotation splittings are also given. Measurement of the high frequency (154–660 GHz) transitions of the parent species are reported by Margulès *et al.* (2010) for the ground state and by Cuisset *et al.* (2013) for the five lowest vibrational states.

As regards the parent species, we extended the spectral investigation to the 59.6–78.4 frequency range and measured some transition lines in the 6–18 GHz frequency range using a higher resolution set-up. The AA transition lines reported by Fliege *et al.* (1983) were fitted using a semi-rigid Hamiltonian in the *S*-reduction and the III^l representations (Watson 1977), suitable for oblate tops such as DMSO, by using the CALPGM suite of programs (Pickett, 1991) and the predictions were

used to search for lines in the higher frequency range. Several μ_b R-type lines with rotational quantum numbers J ranging from 4 to 9, and pseudo-quantum numbers K_a from 0 to 5 and K_c from 0 to 4 were measured. In the same way, starting from the lines measured by Feder *et al.* (1969), the transitions for the monosubstituted ^{34}S and ^{13}C isotopologues were observed in natural abundance and measured in the higher frequency range (accuracy 50 kHz). Some lines both for the parent species and its ^{34}S and ^{13}C monosubstituted isotopologues could be also detected with our cavity-based FTMW spectrometer where they could be measured with a higher accuracy (2 kHz). All newly measured AA lines and those reported in the previous works were analysed in a global semi-rigid fit where each set of lines was weighted accordingly to its measured accuracy. The measured frequencies of the parent species are listed in Table 1 and those of the isotopologues are reported in Table 2, whereas the spectroscopic parameters obtained from the fitting procedure are reported in Table 3.

While the set of AA lines can be fit by using a semi-rigid Hamiltonian, the full set of AA, AE, EA and EE of transition lines needs a global fitting approach which takes into account the coupling effect of the internal rotation of the methyl group on the rotational transitions. For this purpose, the XIAM program (Hartwig and Dreizler, 1996) was used. This program is based on the combined axis method (Woods 1966) and directly supplies the V_3 barrier to internal rotation, the angles between the internal rotation axis and the principal axes and the moment of inertia of the internal top. A total of 195 transitions (including many of those from Fliege *et al.*, 1983) were included in the global fit yielding the values of the rotational constants, the quartic and some sextic centrifugal distortion constants and the internal rotation parameters such as the value of the barrier hindering the motion and the orientation of the internal rotors. The standard deviation of the global fit is 5 kHz which is very close to the best accuracy obtained in the different measurements. In the XIAM program the *S*-reduction can be used but only the I^r representation is available and not the III^l one which would be more suitable for an oblate rotor such as DMSO. In the two representations the centrifugal distortion constants have different values and this is the reason why, in order to compare the AA-fit and the global-fit, we performed different fittings using the two representations for the AA state of the parent species. The comparison of the corresponding spectroscopic parameters reported in Table 4 shows that they are in very good agreement. Predictions from this fit to the 59.6–78.4 GHz region have confirmed that the internal rotation splittings are not resolvable in this region with the absorption spectrometer (resolution 300 kHz).

The obtained results are in good agreement with those reported by Fliege *et al.* (1983) but the accuracy in the determination of the centrifugal distortion constants is better and so is the standard deviation of the fit which is five times better. The experimental results can also be compared to those obtained by in the optimization of the DMSO structure by quantum chemical methods with the Gaussian 16 program (Gaussian, Inc., Wallingford, CT, USA) with the MP2/aug-cc-pVTZ.

The calculated values of the rotational constants ($A = 7000.6$, $B = 6989.0$, $C = 4243.1$ all in MHz) and of the distortion constants in the *S* reduction and III^l representation ($D_J = 6.1$, $D_{JK} = -9.1$, $D_K = 4.1$, $d_1 = -0.25$, $d_2 = -0.23$ all in kHz) are also in good agreement with the experimentally determined ones.

The moment of inertia and orientation of the methyl group was deduced from the structure reported in Feder *et al.* (1969). While the angle $\delta = \angle(ai)$, between the i internal rotation axis of the methyl tops and the a principal axis of overall rotation could be fitted, the ϵ angle between the projection of i on the bc plane and the b axis was fixed to zero as it was undetermined in the fit. This results in experimentally derived values of $\angle(ai) = 32.56(26)/147.44(26)$, $\angle(bi) = 57.44(26)$ (°) for the two methyl tops and a fixed $\angle(ci)$ angle of 90°.

As regards the methyl group internal rotation, the MP2/aug-cc-pVTZ potential energy surface of the methyl torsion around the SC bond in DMSO was calculated by changing the dihedral angle of $\tau = HC - SC$ on the regular grid with $\Delta \tau = 10°$ and is shown in Fig. 2. The calculated data marked in red bullets are well reproduced with the threefold function: $V(\tau) = \frac{1}{2}V_3[1 + \cos(3\tau)]$, which is shown as a green line where $V_3 = 11.6$ kJ mol^{-1}. This value is also in agreement with the experimentally determined value of 12.37(4) kJ mol^{-1}.

The V_3 barrier hindering the methyl torsion in DMSO is thus much higher than the ones found for other molecules which contain a methyl group attached to a sulphur atom such as methylmercaptan

Table 1. *Experimental transition frequencies* ν *and deviations* δν = ν(obs) − ν(calc) *of internal rotation components of DMSO. Calculated frequencies n(calc) are obtained using the spectroscopic parameters listed in* Table 4

J'	K_a'	K_c'	J''	K_a''	K_c''	AA		EE		AE		EA	
						ν (MHz)	$\delta\nu$ (MHz)	ν (MHz)	$\delta\nu$ (MHz)	ν (MHz)	$\delta\nu$ (MHz)	ν (MHz)	$\delta\nu$ (MHz)
4	3	1	4	2	2	7708.102	0.004	7708.102	0.003	7708.102	0.002	7708.102	0.002
3	2	1	3	1	2	7911.502	−0.003	7911.502	−0.001	7911.502	0.000	7911.502	0.000
2	1	1	2	0	2	8080.362	−0.004	8080.362	−0.001	8080.362	0.002	8080.362	0.002
14	13	1	14	12	2	8356.373[a]	0.000	8356.323[a]	−0.001	8356.272[a]	−0.003	8356.272[a]	−0.003
2	2	1	2	1	2	8453.315	−0.007	8453.315	0.001	8453.305	−0.001	8453.305	−0.001
11	11	0	11	10	1	8591.594[a]	−0.001	8591.515[a]	0.000	8591.441[a]	0.007	8591.441[a]	0.006
3	3	1	3	2	2	8644.428	0.000	8644.418	0.000	8644.407	0.000	8644.407	0.000
4	4	1	4	3	2	8900.681	−0.004	8900.674	0.003	8900.658	0.000	8900.658	0.000
15	14	1	15	13	2	9077.647[a]	−0.003	9077.586[a]	−0.001	9077.523[a]	−0.001	9077.523[a]	−0.001
5	5	1	5	4	2	9223.066	−0.002	9223.049	−0.001	9223.031	−0.001	9223.031	−0.001
12	12	0	12	11	1	9797.242[a]	0.000	9797.151[a]	0.002	9797.061[a]	0.006	9797.061[a]	0.004
16	15	1	16	14	2	9953.893[a]	−0.002	9953.817	−0.001	9953.741[a]	0.001	9953.741[a]	0.000
17	16	1	17	15	2	10 979.524[a]	−0.008	10 979.437[a]	−0.003	10 979.350[a]	0.002	10 979.350[a]	0.002
20	18	2	20	17	3	11 065.541[a]	0.003	11 065.509[a]	0.003	11 065.476	0.002	11 065.476	0.002
13	13	0	13	12	1	11 081.929[a]	−0.006	11 081.830[a]	−0.001	11 081.729[a]	0.004	11 081.729[a]	0.002
9	9	1	9	8	2	11 187.003[a]	0.005	11 186.959[a]	0.004	11 186.916[a]	0.003	11 186.916[a]	0.003
1	1	1	0	0	0	11 255.349	−0.005	11 255.349	−0.002	11 255.349	0.001	11 255.349	0.001
21	19	2	21	18	3	11 592.719[a]	0.003	11 592.674[a]	0.004	11 592.628[a]	0.004	11 592.628[a]	0.004
18	17	1	18	16	2	12 142.142[a]	−0.008	12 142.043[a]	−0.002	12 141.941[a]	0.002	12 141.941[a]	0.002
22	20	2	22	19	3	12 299.804[a]	0.005	12 299.745[a]	0.006	12 299.685[a]	0.006	12 299.685[a]	0.006
14	14	0	14	13	1	12 422.368[a]	0.001	12 422.251[a]	−0.002	12 422.134[a]	−0.002	12 422.134[a]	−0.005
23	21	2	23	20	3	13 186.345[a]	0.002	13 186.264[a]	−0.006	13 186.190[a]	−0.006	13 186.190[a]	−0.006
19	18	1	19	17	2	13 422.951[a]	0.000	13 422.830[a]	−0.003	13 422.717[a]	0.002	13 422.717[a]	0.002
4	2	2	4	1	3	13 724.668	−0.006	13 724.668	0.002	13 724.668	0.010	13 724.668	0.010
3	1	2	3	0	3	13 755.597	0.000	13 755.597	0.009	13 755.574	−0.005	13 755.574	−0.005
3	2	2	3	1	3	13 777.060	0.004	13 777.041	−0.007	13 777.035	−0.003	13 777.035	−0.003
4	3	2	4	2	3	13 788.443	−0.007	13 788.443	0.003	13 788.433	0.002	13 788.433	0.002
15	15	0	15	14	1	13 795.465[a]	−0.001	13 795.345[a]	0.002	13 795.225[a]	0.008	13 795.225[a]	0.004

5	4	2	5	3	3	13 811.543	−0.001	13 811.533	0.000	13 811.522	−0.001	13 811.522	−0.001
24	22	2	24	21	3	14 245.341[a]	−0.003	14 245.254[a]	−0.003	14 245.165[a]	−0.006	14 245.165[a]	−0.006
20	19	1	20	18	2	14 798.162[a]	−0.005	14 798.038[a]	−0.001	14 797.915[a]	0.006	14 797.915[a]	0.005
14	14	1	14	13	2	15 091.974[a]	0.009	15 091.878[a]	−0.001	15 091.786[a]	−0.008	15 091.786[a]	−0.005
16	16	0	16	15	1	15 180.655[a]	−0.001	15 180.529[a]	0.003	15 180.403[a]	0.011	15 180.403[a]	0.005
25	23	2	25	22	3	15 462.669[a]	−0.004	15 462.575[a]	0.000	15 462.478[a]	0.001	15 462.478[a]	0.001
15	15	1	15	14	2	16 036.379[a]	0.010	16 036.273[a]	−0.001	16 036.174[a]	−0.007	16 036.174[a]	−0.002
21	20	1	21	19	2	16 241.210[a]	0.000	16 241.072[a]	−0.001	16 240.937[a]	0.001	16 240.937[a]	0.000
17	17	0	17	16	1	16 561.411[a]	0.000	16 561.549[a]	0.002	16 561.272[a]	0.002	16 561.272[a]	−0.008
26	24	2	26	23	3	16 817.381[a]	0.001	16 817.277[a]	0.003	16 817.169[a]	0.002	16 817.169[a]	0.002
16	16	1	16	15	2	17 023.943[a]	0.012	17 023.827[a]	0.001	17 023.710[a]	−0.015	17 023.710[a]	−0.008
17	16	2	17	15	3	17 115.125[a]	0.006	17 115.057[a]	−0.002	17 114.993[a]	−0.006	17 114.993[a]	−0.005
22	21	1	22	20	2	17 725.185[a]	0.004	17 725.040[a]	0.002	17 724.896[a]	0.002	17 724.896[a]	0.000
18	17	2	18	16	3	17 778.453[a]	0.005	17 778.380[a]	0.001	17 778.305[a]	−0.006	17 778.305[a]	−0.006
18	18	0	18	17	1	17 926.735[a]	0.002	17 926.594[a]	0.002	17 926.446[a]	0.001	17 926.446[a]	−0.013
19	19	0	19	18	1	19 269.635[a]	−0.013	19 269.507[a]	0.003	19 269.381[a]	0.031	19 269.381[a]	0.011
5	3	2	4	4	1	60 694.130	0.011	60 694.130	0.013	60 694.130	0.014	60 694.130	0.014
7	0	7	6	1	6	61 815.380	0.024	61 815.380	0.026	61 815.380	0.028	61 815.380	0.028
5	4	2	4	3	1	62 100.400	−0.032	62 100.400	−0.012	62 100.400	0.009	62 100.400	0.009
4	3	1	3	2	2	63 435.480	−0.005	63 435.480	0.008	63 435.480	0.021	63 435.480	0.021
6	2	4	5	3	3	64 394.850	0.012	64 394.850	0.021	64 394.850	0.030	64 394.850	0.030
6	3	4	5	2	3	64 397.520	−0.001	64 397.520	0.009	64 397.520	0.018	64 397.520	0.018
4	4	1	3	1	2	64 714.030	−0.022	64 714.030	0.007	64 714.030	0.037	64 714.030	0.037
7	1	6	6	2	5	67 323.270	−0.021	67 323.270	−0.015	67 323.270	−0.010	67 323.270	−0.010
5	5	1	4	4	0	67 887.270	−0.039	67 887.270	−0.012	67 887.270	0.016	67 887.270	0.016
5	4	1	4	3	1	69 439.500	−0.008	69 439.500	0.007	69 439.500	0.021	69 439.500	0.021
4	2	2	3	1	3	69 504.440	−0.002	69 504.440	0.020	69 504.440	0.043	69 504.440	0.043
4	3	2	3	0	3	69 568.990	0.026	69 568.990	0.050	69 568.990	0.074	69 568.990	0.074
5	3	2	4	2	2	69 659.180	−0.052	69 659.180	−0.036	69 659.180	−0.019	69 659.180	−0.019
5	2	3	4	1	3	69 719.100	0.045	69 719.100	0.063	69 719.100	0.081	69 719.100	0.081
5	3	3	4	2	3	69 721.030	0.021	69 721.030	0.039	69 721.030	0.057	69 721.030	0.057
5	1	4	4	0	4	69 725.900	0.002	69 725.900	0.020	69 725.900	0.039	69 725.900	0.039
5	4	2	4	3	2	69 744.140	0.037	69 744.140	0.056	69 744.140	0.074	69 744.140	0.074

(*Continued*)

Table 1. (*Continued.*)

J'	K_a'	K_c'	J''	K_a''	K_c''	AA		EE		AE		EA	
						v (MHz)	δv (MHz)	v (MHz)	δv (MHz)	v (MHz)	δv (MHz)	v (MHz)	δv (MHz)
5	5	0	4	4	0	69 818.640	−0.032	69 818.640	−0.012	69 818.640	0.008	69 818.640	0.008
6	3	3	5	4	2	69 839.700	−0.021	69 839.700	−0.009	69 839.700	0.002	69 839.700	0.002
6	4	3	5	3	2	69 996.800	−0.025	69 996.800	−0.011	69 996.800	0.004	69 996.800	0.004
5	5	1	4	4	1	70 066.450	−0.036	70 066.450	−0.013	70 066.450	0.010	70 066.450	0.010
8	0	8	7	1	7	70 252.080	−0.003	70 252.080	−0.001	70 252.080	0.001	70 252.080	0.001
8	1	8	7	0	7	70 252.080	−0.003	70 252.080	−0.001	70 252.080	0.001	70 252.080	0.001
5	5	0	4	4	1	71 997.850	0.002	71 997.850	0.017	71 997.850	0.033	71 997.850	0.033
8	1	7	7	2	6	75 759.820	−0.003	75 759.820	0.002	75 759.820	0.008	75 759.820	0.008
6	5	2	5	4	1	76 360.180	−0.017	76 360.180	0.011	76 360.180	0.039	76 360.180	0.039
5	4	1	4	3	2	77 083.190	0.011	77 083.190	0.024	77 083.190	0.036	77 083.190	0.036
7	3	4	6	4	3	78 339.690	−0.094	78 339.690	−0.081	78 339.690	−0.069	78 339.690	−0.069
7	4	4	6	3	3	78 347.780	−0.088	78 347.780	−0.075	78 347.780	−0.062	78 347.780	−0.062
9	0	9	8	1	8	78 688.580	−0.005	78 688.580	−0.003	78 688.580	−0.001	78 688.580	−0.001
5	5	1	4	2	2	79 031.560	−0.039	79 031.560	−0.001	79 031.560	0.037	79 031.560	0.037

[a]From E. Fliege *et al.* (1983).

Table 2. *Experimental transition frequencies of AA lines of DMSO (^{34}S) and DMSO (^{13}C)*

Transition $J'_{K'_a K'_c} \leftarrow J''_{K''_a K''_c}$	^{34}S ν (MHz)	$\delta\nu$ (MHz)	^{13}C ν (MHz)	$\delta\nu$ (MHz)
$9_{8,1} \leftarrow 9_{7,2}$	6820.25[a]	0.052		
$10_{9,1} \leftarrow 10_{8,2}$	6843.35[a]	−0.065		
$6_{5,1} \leftarrow 6_{4,2}$	7206.288[a]	0.047	6792.723[a]	−0.032
$12_{11,1} \leftarrow 12_{10,2}$	7221.04[a]	0.017		
$5_{4,1} \leftarrow 5_{3,2}$	7416.028[a]	−0.065	6832.64[a]	−0.001
$4_{3,1} \leftarrow 4_{2,2}$	7629.257[a]	−0.001	7060.448[a]	0.007
$3_{2,1} \leftarrow 3_{1,2}$	7825.496[a]	0.012	7389.72[a]	0.002
$2_{1,1} \leftarrow 2_{0,2}$	7987.797[a]	−0.003	7730.1[a]	0.026
$2_{2,1} \leftarrow 2_{1,2}$	8345.136[a]	−0.003	8621.721[a]	0.005
$3_{3,1} \leftarrow 3_{2,2}$	8528.119[a]	0.016	9095.719[a]	0.026
$4_{4,1} \leftarrow 4_{3,2}$	8773.47[a]	0.061	9734.62[a]	−0.012
$7_{7,1} \leftarrow 7_{6,2}$	9892.1	−0.03		
$5_{5,1} \leftarrow 5_{4,2}$			10 541.04[a]	0.107
$6_{6,1} \leftarrow 6_{5,2}$			11 513.85[a]	0.003
$9_{9,1} \leftarrow 9_{8,2}$	10 961.82	0.012		
$1_{1,1} \leftarrow 0_{0,0}$	11 216.6301	0	11 136.86[a]	−0.002
$1_{0,1} \leftarrow 0_{0,0}$			10 831.07	0.001
$2_{1,2} \leftarrow 1_{0,1}$			19 399.75[a]	0.001
$2_{2,1} \leftarrow 1_{1,0}$	25 214.893[a]	0.003	25 147.49[a]	−0.045
$3_{1,2} \leftarrow 2_{2,1}$	33 268.234[a]	−0.013		
$3_{2,2} \leftarrow 2_{1,1}$	33 649.641[a]	0.017		
$5_{3,2} \leftarrow 4_{4,1}$	60 483.86	0.003		
$7_{0,7} \leftarrow 6_{1,6}$	61 763.33	−0.005	60 555.67	0.012
$7_{1,7} \leftarrow 6_{0,6}$	61 763.33	−0.005	60 555.67	0.012
$4_{3,1} \leftarrow 3_{2,2}$	63 083.05	−0.019		
$7_{1,6} \leftarrow 6_{2,5}$	67 204.55	−0.014	65 989.46	0.052
$7_{2,6} \leftarrow 6_{1,5}$			65 989.46	0.025
$6_{3,3} \leftarrow 5_{4,2}$	69 594.79	0.012		
$6_{4,3} \leftarrow 5_{3,2}$	69 740.68	0.03		
$8_{0,8} \leftarrow 7_{1,7}$	70 197.38	−0.003	68 817.84	0.057
$8_{1,8} \leftarrow 7_{0,7}$	70 197.38	−0.003	68 817.84	0.057
$5_{5,0} \leftarrow 4_{4,1}$	71 633.93	0.023		
$7_{2,5} \leftarrow 6_{3,4}$	72 646.24	0.049		
$7_{3,5} \leftarrow 6_{2,4}$	72 646.24	−0.018		
$6_{4,2} \leftarrow 5_{5,1}$	73 924.52	−0.007		
$8_{1,7} \leftarrow 7_{2,6}$	75 638.42	−0.005	74 251.06	−0.033
$8_{2,7} \leftarrow 7_{1,6}$	75 638.42	−0.005	74 251.06	−0.034
$6_{5,2} \leftarrow 5_{4,1}$	76 003.83	−0.041		
$7_{3,4} \leftarrow 6_{4,3}$	78 087.66	−0.017		
$7_{4,4} \leftarrow 6_{3,3}$	78 094.98	0.014		
$9_{0,9} \leftarrow 8_{1,8}$	78 631.21	0.008	77 079.66	−0.04
$9_{1,9} \leftarrow 8_{0,8}$	78 631.21	0.008	77 079.66	−0.04

[a]From Feder *et al.* (1969).

Table 3. *Spectroscopic parameters for the AA state of DMSO, DMSO (^{34}S) and DMSO (^{13}C) (S-reduction, III^l representation)*

	Parent	^{34}S	^{13}C
A (MHz)	7036.5835(10)[a]	6999.1925(41)	7005.4022(56)
B (MHz)	6910.8300(10)	6878.7479(44)	6699.6175(54)
C (MHz)	4218.7766(10)	4217.4471(41)	4131.4659(47)
D_J (kHz)	6.083(20)	5.962(78)	5.67(20)
D_{JK} (kHz)	−8.9142(92)	−8.67(23)	−8.13(50)
D_K (kHz)	4.024(42)	3.88(16)	3.54(30)
d_1 (kHz)	−0.16378(14)	−0.218(15)	[0][b]
d_2 (kHz)	−0.271512(59)	−0.292(36)	[0]
H_{JK}[c] (Hz)	−0.104(31)	[0]	[0]
H_{KJ} (Hz)	2.99(72)	[0]	[0]
H_K (Hz)	−2.62(72)	[0]	[0]
h_1 (Hz)	−0.00176(22)	[0]	[0]
h_2 (Hz)	0.00074(15)	[0]	[0]
h_3 (Hz)	−0.001159(48)	[0]	[0]
N[d]	75	37	24
σ[e] (kHz)	21	28	35

[a]Standard error in parenthesis in units of the last digits.
[b]Constants fixed to zero as they result undetermined.
[c]H_J is undetermined from the fit and has been fixed to zero.
[d]Number of transitions.
[e]Standard deviation of the fit.

(5.31(1) kJ mol^{-1}) (Kojima, 1960), DMS (8.8030(5) kJ mol^{-1}) (Pierce and Hayashi, 1961; Jabri *et al.*, 2016) and dimethyl disulphide (6.44 kJ mol^{-1}) (Hartwig *et al.*, 1995). This could be due to electronic effects related to the presence of the oxygen atom or to an attractive interaction between the oxygen atoms and the methyl hydrogens which can increase the barrier to internal rotation of this group.

Based on the obtained fittings, an overall prediction in the 0–1000 GHz range calculated at five different temperatures which could be found in different astronomical objects is reported in Fig. 3. While the measurements are performed up to 78.4 GHz, the predictions are quite reliable in the adjacent frequency range covered by band 3 of ALMA (84–116 GHz) for lines with rotational quantum number J less than 12. In the bottom panel of Fig. 3, an expanded view of this frequency range can be found where the frequencies and intensities of main lines calculated at different temperatures are reported. Here, we can see that the most intense transitions are somehow the same ones at different temperatures. Moreover, a thorough analysis of the predictions showed that in this frequency range the internal rotation splittings are units or tens of kilohertz thus, even if very small, they might be observable at the resolution of some astronomical surveys which can show line-widths as low as 10 kHz (see for example Loomis *et al.*, 2021). For a quantitative analysis, the predicted frequencies with their uncertainties and intensities at different temperature are reported in Table 5 while the internal rotation components are given as supplementary material (Table S1). The AA predicted frequencies from our fit are accurate within ten kilohertz as assessed by performing some fits which included lines measured at higher frequencies by Margulès *et al.* (2010).

Conclusions

In this work, rotational spectroscopy coupled to supersonic expansions has been exploited to characterize the rotational spectrum of DMSO and its ^{34}S and ^{13}C monosubstituted isotopologues. The lines were measured in the 59.6–78.4 GHz frequency range with an absorption spectrometer while a cavity-

Table 4. *Spectroscopic parameters for the global fit of DMSO compared to the fitting of AA lines both in* I^r *representation*

	Global fit	AA fit
A (MHz)	7036.57930(48)[a]	7036.5809(10)
B (MHz)	6911.09686(61)	6910.8300(10)
C (MHz)	4218.51423(57)	4218.77916(91)
D_J (kHz)	3.4579(77)	3.458(16)
D_{JK} (kHz)	−0.9319(10)	−0.9285(16)
D_K (kHz)	3.7654 (24)	3.7665(48)
d_1 (kHz)	−1.4503(29)	−1.4550(60)
d_2 (kHz)	−0.2956(14)	−0.2921(29)
H_{JK}[b] (Hz)	0.039(10)	0.4117(59)
H_{KJ} (Hz)	−0.114(10)	−0.1135(13)
H_K (Hz)	0.087(20)	0.0827(17)
V_3 (kJ mol^{-1})	12.38(30)	
I_α (μÅ)	3.146[c]	
δ [d] (rad)	0.5683(46)/2.5733(46)	
$\angle(ai)$[e] (°)	32.56(26)/147.44(26)	
$\angle(bi)$ (°)	57.44(26)	
$\angle(ci)$ (°)	90	
N[f]	195	75
σ[g] (kHz)	4.4	20

[a]Standard error in parenthesis in units of the last digits.

[b]H_J is undetermined from the fit and has been fixed to zero.

[c]Fixed to the value obtained from the r_z structure (Feder *et al.*, 1969).

[d]$\delta = \angle(ai)$, where *i* is the internal rotation axis of the methyl tops. ϵ (angle between the projection of *i* on the *bc* plane and the *b* axis) fixed to zero as undetermined from the fit.

[e]Derived parameters.

[f]Number of measured transitions in the fit.

[g]Standard deviation of the fit.
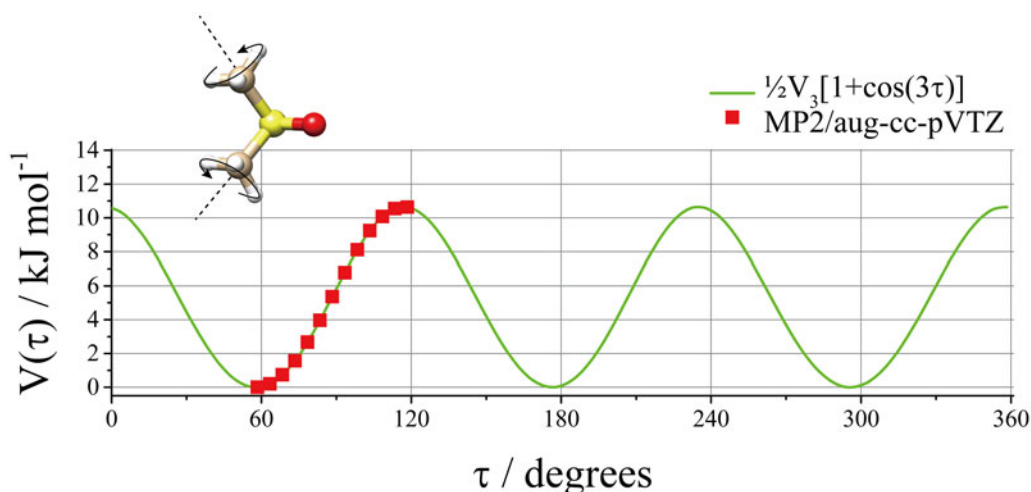
Fig. 2. Ab initio *(MP2-aug-cc-pVTZ) methyl internal rotational potential energy surface for DMSO.*
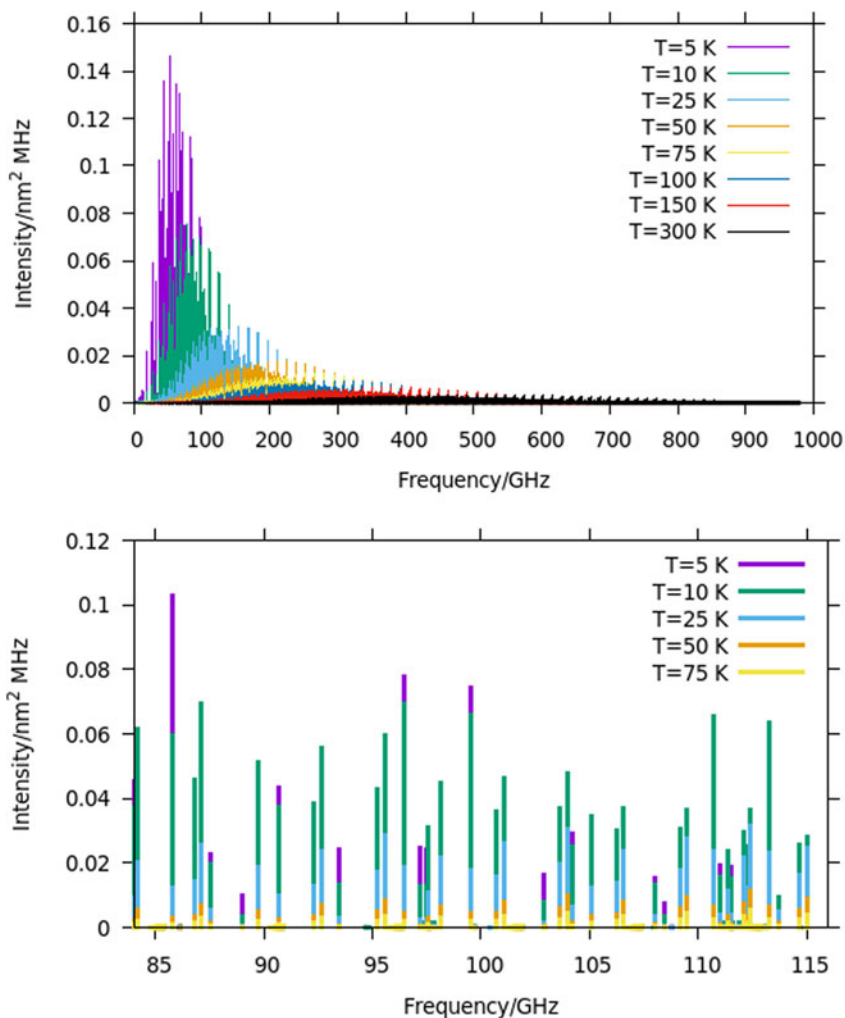
Fig. 3. *Top panel: Spectral predictions in the 0–1000 GHz frequency range for DMSO at eight different temperatures. Bottom panel: Expanded spectral window overlapping with the frequency region covered by the ALMA telescope (band 3, 84–116 GHz).*

based FTMW spectrometer has allowed to re-measure DMSO transitions split by the methyl rotor internal rotation in the 6–18 GHz region with unprecedented high resolution and accuracy. A global fit of 195 lines has allowed for an accurate modelling of the internal rotation lines and the accurate determination of the spectroscopic parameters obtained by applying appropriate models. The molecular parameters related to the geometry of the molecule or its internal dynamics (methyl torsional barrier) could also be used to model the ro-vibrational spectrum of DMSO.

The measured rotational lines can be confidently used for the analysis of astronomical surveys for the unequivocal identification of DMSO and its isotopologues in different astronomical environments such as the interstellar medium, star-forming regions and planetary atmospheres. A natural place where one would try is astronomical objects where organic molecules containing sulphur have been detected. For example, in giant molecular clouds like Sagittarius B2 (Müller *et al.*, 2016) or protostars (Majumdar *et al.*, 2016). Tentative detection of sulphur-containing molecules has also been attempted in prestellar cores (Maris *et al.*, 2019) and molecular clouds (Song *et al.*, 2022). Besides remote sensing, the value of rotational spectroscopy as a means of exact identification

Table 5. *Selected predicted transitions in the Alma band 3 spectral region (84–116 GHz): predicted frequency (MHz), estimated uncertainty (MHz) and base 10 logarithm of the integrated intensity in units of nm^2 MHz at different temperatures*

J'	K_a'	K_c'	J''	K_a''	K_c''	v (MHz)	err	5 K	10 K	25 K	50 K	75 K	100 K	150 K	300 K
5	2	3	4	1	4	88 994.71[a]	0.01	−1.9985	−2.4665	−3.2876	−3.9817	−4.4025	−4.7051	−5.1356	−5.8786
5	3	3	4	0	4	8 8997.32	0.01	−1.9985	−2.4665	−3.2876	−3.9817	−4.4025	−4.7051	−5.1356	−5.8786
6	2	4	5	1	5	108 450.81	0.02	−2.1274	−2.4862	−3.2401	−3.9117	−4.3249	−4.6237	−5.0505	−5.7896
6	3	4	5	0	5	108 450.89	0.02	−2.1274	−2.4862	−3.2401	−3.9117	−4.3249	−4.6237	−5.0505	−5.7896
6	3	3	5	2	4	102 922.66	0.01	−1.7904	−2.1018	−2.8279	−3.4902	−3.9003	−4.1976	−4.6228	−5.3605
6	4	3	5	1	4	102 930.48	0.01	−1.7904	−2.1018	−2.8279	−3.4902	−3.9003	−4.1976	−4.6228	−5.3605
6	4	2	5	3	3	97 215.65	0.01	−1.6107	−1.8865	−2.5916	−3.2470	−3.6549	−3.9510	−4.3751	−5.1116
6	5	2	5	2	3	97 513.39	0.01	−1.6150	−1.8906	−2.5955	−3.2509	−3.6587	−3.9548	−4.3789	−5.1154
6	5	1	5	4	2	90 678.12	0.01	−1.4138	−1.6661	−2.3576	−3.0086	−3.4149	−3.7104	−4.1337	−4.8695
6	6	1	5	3	2	93 461.02	0.01	−1.6182	−1.8686	−2.5587	−3.2092	−3.6154	−3.9107	−4.3340	−5.0696
6	6	0	5	5	1	85 756.03	0.01	−0.9873	−1.2245	−1.9073	−2.5554	−2.9608	−3.2557	−3.6786	−4.4138
7	5	3	6	4	2	84 037.91	0.02	−1.3449	−1.4289	−2.0198	−2.6373	−3.0325	−3.3224	−3.7402	−4.4703
7	5	2	6	4	3	110 987.70	0.02	−1.7147	−1.8053	−2.3981	−3.0160	−3.4112	−3.7011	−4.1189	−4.8491
7	5	2	6	6	1	87 523.48	0.02	−1.6430	−1.7034	−2.2800	−2.8927	−3.2863	−3.5753	−3.9923	−4.7217
7	6	2	6	3	3	111 517.39	0.02	−1.7235	−1.8137	−2.4063	−3.0241	−3.4193	−3.7091	−4.1269	−4.8571
7	6	2	6	5	1	90 678.96	0.02	−1.3649	−1.4283	−2.0064	−2.6195	−3.0133	−3.3024	−3.7194	−4.4489
7	6	1	6	5	2	104 224.74	0.02	−1.5342	−1.6013	−2.1805	−2.7939	−3.1877	−3.4769	−3.8939	−4.6234
7	7	1	6	4	2	108 022.55	0.02	−1.8188	−1.8834	−2.4610	−3.0737	−3.4673	−3.7563	−4.1733	−4.9026
7	7	1	6	6	0	96 447.56	0.02	−1.1095	−1.1592	−1.7287	−2.3389	−2.7316	−3.0203	−3.4368	−4.1658
7	7	0	6	6	1	99 517.15	0.02	−1.1302	−1.1809	−1.7507	−2.3611	−2.7538	−3.0425	−3.4590	−4.1880
8	3	5	7	4	4	86 776.82	0.03	−1.3941	−1.3408	−1.8491	−2.4391	−2.8251	−3.1104	−3.5236	−4.2491
8	4	5	7	3	4	86 777.10	0.03	−1.3941	−1.3408	−1.8491	−2.4391	−2.8251	−3.1104	−3.5236	−4.2491
8	4	4	7	5	3	92 283.79	0.03	−1.5119	−1.4140	−1.8952	−2.4760	−2.8590	−3.1427	−3.5544	−4.2784
8	5	4	7	4	3	92 304.08	0.03	−1.5115	−1.4136	−1.8948	−2.4756	−2.8586	−3.1423	−3.5540	−4.2780
8	5	3	7	6	2	97 569.92	0.03	−1.6385	−1.5072	−1.9681	−2.5421	−2.9227	−3.2053	−3.6158	−4.3387
8	6	3	7	5	2	98 134.39	0.03	−1.6196	−1.4890	−1.9501	−2.5242	−2.9049	−3.1875	−3.5981	−4.3210
8	6	2	7	7	1	100 702.46	0.03	−1.9888	−1.8341	−2.2806	−2.8498	−3.2288	−3.5106	−3.9203	−4.6424
8	7	2	7	6	1	105 053.53	0.03	−1.6154	−1.4645	−1.9130	−2.4828	−2.8620	−3.1439	−3.5537	−4.2759
8	8	1	7	7	0	110 743.18	0.03	−1.3509	−1.1854	−1.6246	−2.1912	−2.5694	−2.8507	−3.2600	−3.9816

(*Continued*)

Table 5. (*Continued.*)

J′	Kₐ′	K꜀′	J″	Kₐ″	K꜀″	ν (MHz)	err	5 K	10 K	25 K	50 K	75 K	100 K	150 K	300 K
8	8	0	7	7	1	113 295.03	0.03	−1.3614	−1.1968	−1.6364	−2.2031	−2.5813	−2.8627	−3.2719	−3.9936
9	1	8	8	2	7	84 196.21	0.03	−1.3041	−1.2098	−1.6937	−2.2756	−2.6589	−2.9428	−3.3546	−4.0789
9	2	8	8	1	7	84 196.21	0.03	−1.3041	−1.2098	−1.6937	−2.2756	−2.6589	−2.9428	−3.3546	−4.0789
9	2	7	8	3	6	89 703.64	0.04	−1.4647	−1.2912	−1.7273	−2.2931	−2.6711	−2.9523	−3.3615	−4.0831
9	3	7	8	2	6	89 703.64	0.04	−1.4647	−1.2912	−1.7273	−2.2931	−2.6711	−2.9523	−3.3615	−4.0831
9	3	6	8	4	5	95 211.68	0.04	−1.6103	−1.3692	−1.7643	−2.3164	−2.6898	−2.9688	−3.3756	−4.0949
9	4	6	8	3	5	95 211.69	0.04	−1.6103	−1.3692	−1.7643	−2.3164	−2.6898	−2.9688	−3.3756	−4.0949
9	4	5	8	5	4	100 722.41	0.04	−1.7420	−1.4449	−1.8059	−2.3466	−2.7162	−2.9932	−3.3982	−4.1156
9	5	5	8	4	4	100 723.27	0.04	−1.7420	−1.4448	−1.8059	−2.3466	−2.7162	−2.9932	−3.3982	−4.1155
9	5	4	8	6	3	106 225.61	0.05	−1.8634	−1.5218	−1.8558	−2.3874	−2.7539	−3.0294	−3.4329	−4.1487
9	6	4	8	5	3	106 270.35	0.05	−1.8625	−1.5210	−1.8550	−2.3866	−2.7531	−3.0287	−3.4321	−4.1479
9	6	3	8	7	2	111 366.12	0.05	−2.0015	−1.6268	−1.9404	−2.4652	−2.8294	−3.1037	−3.5060	−4.2207
9	7	3	8	6	2	112 299.05	0.05	−1.9700	−1.5963	−1.9105	−2.4354	−2.7997	−3.0741	−3.4764	−4.1911
9	7	2	8	8	1	113 702.61	0.05	−2.4217	−2.0231	−2.3222	−2.8421	−3.2047	−3.4782	−3.8797	−4.5935
10	0	10	9	1	9	87 124.89	0.09	−1.3344	−1.1598	−1.5953	−2.1610	−2.5389	−2.8202	−3.2293	−3.9508
10	1	10	9	0	9	87 124.89	0.09	−1.3344	−1.1598	−1.5953	−2.1610	−2.5389	−2.8202	−3.2293	−3.9508
10	1	9	9	2	8	92 632.35	0.06	−1.5333	−1.2565	−1.6304	−2.1755	−2.5466	−2.8243	−3.2300	−3.9481
10	2	9	9	1	8	92 632.35	0.06	−1.5333	−1.2565	−1.6304	−2.1755	−2.5466	−2.8243	−3.2300	−3.9481
10	2	8	9	3	7	98 139.46	0.06	−1.7152	−1.3479	−1.6671	−2.1938	−2.5587	−2.8335	−3.2361	−3.9511
10	3	8	9	2	7	98 139.46	0.06	−1.7152	−1.3479	−1.6671	−2.1938	−2.5587	−2.8335	−3.2361	−3.9511
10	3	7	9	4	6	103 646.75	0.06	−1.8803	−1.4341	−1.7054	−2.2162	−2.5758	−2.8478	−3.2478	−3.9601
10	4	7	9	3	6	103 646.75	0.06	−1.8803	−1.4341	−1.7054	−2.2162	−2.5758	−2.8478	−3.2478	−3.9601
10	4	6	9	5	5	109 155.51	0.06	−2.0294	−1.5157	−1.7462	−2.2432	−2.5982	−2.8680	−3.2657	−3.9757
10	5	6	9	4	5	109 155.54	0.06	−2.0294	−1.5157	−1.7462	−2.2432	−2.5982	−2.8680	−3.2657	−3.9757
10	5	5	9	6	4	114 668.75	0.07	−2.1639	−1.5944	−1.7909	−2.2765	−2.6277	−2.8955	−3.2913	−3.9994
10	6	5	9	5	4	114 670.99	0.07	−2.1638	−1.5943	−1.7908	−2.2765	−2.6277	−2.8955	−3.2913	−3.9994
11	0	11	10	1	10	95 560.94	0.18	−1.5889	−1.2257	−1.5476	−2.0753	−2.4405	−2.7154	−3.1182	−3.8334
11	1	11	10	0	10	95 560.94	0.18	−1.5889	−1.2257	−1.5476	−2.0753	−2.4405	−2.7154	−3.1182	−3.8334
11	1	10	10	2	9	101 068.26	0.12	−1.8106	−1.3340	−1.5873	−2.0921	−2.4497	−2.7208	−3.1197	−3.8311
11	2	10	10	1	9	101 068.26	0.12	−1.8106	−1.3340	−1.5873	−2.0921	−2.4497	−2.7208	−3.1197	−3.8311
11	2	9	10	3	8	106 575.08	0.10	−2.0143	−1.4357	−1.6275	−2.1117	−2.4624	−2.7300	−3.1255	−3.8335

11	3	9	10	2	8	106 575.08	0.10	−2.0143	−1.4357	−1.6275	−2.1117	−2.4624	−2.7300	−3.1255	−3.8335
11	3	8	10	4	7	112 081.81	0.09	−2.2000	−1.5312	−1.6683	−2.1341	−2.4788	−2.7433	−3.1358	−3.8406
11	4	8	10	3	7	112 081.81	0.09	−2.2000	−1.5312	−1.6683	−2.1341	−2.4788	−2.7433	−3.1358	−3.8406

[a]The intensities were calculated using the partition function from the semirigid approximation. The following values were used: $Q(5\ K) = 133.3339$, $Q(10\ K) = 374.6724$, $Q(25) = 1475.3676$, $Q(50) = 4168.2031$, $Q(75) = 7655.3187$, $Q(100) = 11\ 785.2365$, $Q(150) = 21\ 651.4854$, $Q(300) = 61\ 250.6707$.

and quantification of molecules could also be exploited in the search of biosignatures using instruments for *in situ* analysis.

Author contributions. The manuscript was written through contributions of all authors. All authors have given approval to the final version of the manuscript.

References

Akkök ÇA, Liseth K, Hervig T, Ryningen A, Bruserud ØH and Ersvær E (2009) Use of different DMSO concentrations for cryopreservation of autologous peripheral blood stem cell grafts does not have any major impact on levels of leukocyte-and platelet-derived soluble mediators. *Cytotherapy* **11**, 749–760.

Balle TJ and Flygare WH (1981) Fabry–Perot cavity pulsed Fourier transform microwave spectrometer with a pulsed nozzle particle source. *Review of Scientific Instruments* **52**, 33–45.

Burrows AS (2014) Spectra as windows into exoplanet atmospheres. *Proceedings of the National Academy of Sciences of the United States of America* **111**, 12601–12609.

Calabrese C, Maris A, Evangelisti L, Favero LB, Melandri S and Caminati W (2013) Keto-enol tautomerism and conformational landscape of 1,3-cyclohexanedione from its free jet millimeter-wave absorption spectrum. *Journal of Physical Chemistry A* **117**, 13712–13718.

Calabrese C, Vigorito A, Feng G, Favero LB, Maris A, Melandri S, Geppert WD and Caminati W (2014) Laboratory rotational spectrum of acrylic acid and its isotopologues in the 6–18.5 GHz and 52–74.4 GHz frequency ranges. *Journal of Molecular Spectroscopy* **295**, 37–43.

Calabrese C, Vigorito A, Maris A., Mariotti S, Fathi P, Geppert WD and Melandri S (2015) Millimeter wave spectrum of the weakly bound complex $CH_2=CHCN \cdot H_2O$: structure, dynamics, and implications for astronomical search. *Journal of Physical Chemistry A* **119**, 11674–11682.

Calabrese C, Gou Q, Maris A, Melandri S and Caminati W (2016) Conformational equilibrium and internal dynamics of E-anethole: a rotational study. *The Journal of Physical Chemistry B* **120**, 6587–6591.

Caminati W, Evangelisti L, Feng G, Giuliano BM, Gou Q, Melandri S and Grabow J-U (2016) On the Cl···C halogen bond: a rotational study of CF_3Cl–CO. *Physical Chemistry Chemical Physics* **18**, 17851–17855.

CDMS (2001) The Cologne Database for Molecular Spectroscopy (n.d.). Available at www.astro.uni-koeln.de/cdms/molecules.

Cuisset A, Drumel M-AM, Hindle F, Mouret G and Sadovskií DA (2013) Rotational structure of the five lowest frequency fundamental vibrational states of dimethylsulfoxide. *Chemical Physics Letters* **586**, 10–15.

Des Marais DJ, Harwit MO, Jucks KW, Kasting JF, Lin DNC, Lunine JI, Schneider J, Seager S, Traub WA and Woolf NJ (2002) Remote sensing of planetary properties and biosignatures on extrasolar terrestrial planets. *Astrobiology* **2**, 153–181.

Dindić C and Nguyen HVL (2021) Microwave spectrum of two-top molecule: 2-acetyl-3-methylthiophene. *Chemphyschem* **22.23**, 2420–2428

Domagal-Goldman SD, Meadows VS, Claire MW and Kasting JF (2011) Using biogenic sulfur gases as remotely detectable biosignatures on anoxic planets. *Astrobiology* **11**, 419–441.

Dreizler H (1961) Gruppentheoretische betrachtungen zu den mikrowellenspektren von molekülen mit zwei behindert drehbaren dreizählig-symmetrischen molekülgruppen. *Zeitschrift für* Naturfor*sch A* **16**, 1354–1367.

Dreizler H and Dendl G (1964) Rotations spektrum, r_0-struktur und dipolmoment von dimethvlsulfoxyd. *Zeitschrift für Naturforsch A* **19**, 512–514.

Dreizler H and Dendl G (1965a) Erfahrungen bei der analyse der zentrifugalaufweitung in rotationsspektren I. Dimethylsulfoxyd. *Zeitschrift für Naturforsch A* **20**, 30–37.

Dreizler H and Dendl G (1965b) Bestimmung des Hinderungspotentials der internen Rotation aus dem Mikrowellenspektrum von Dimethylsulfoxyd. *Zeitschrift für Naturforsch A* **20**, 1431–1440.

Evangelisti L, Perez C, Seifert NA, Pate BH, Dehghany M, Moazzen-Ahmadi N and McKellar ARW (2015) Theory vs. experiment for molecular clusters: spectra of OCS trimers and tetramers. *The Journal of Chemical Physics* **142**, 104309.

Favero LB, Giuliano BM, Maris A, Melandri S, Ottaviani P, Velino B and Caminati W (2010) Features of the C-H…N weak hydrogen bond and internal dynamics in pyridine-CHF_3. *Chemistry (Weinheim an Der Bergstrasse, Germany)* **16**, 1761–1764.

Feder W, Dreizler H, Rudolph HD and Typke V (1969) rs-Struktur von dimethylsulfoxid im vergleich zur r0-struktur. *Zeitschrift für Naturforsch A* **24**, 266–278.

Fliege E, Dreizler H and Typke V (1983) Centrifugal distortion and ground state internal rotation analysis of the microwave spectrum of dimethylsulfoxide. *Zeitschrift für Naturforsch A* **38**, 668–675.

Grabow JU, Stahl W and Dreizler H (1996) A multioctave coaxially oriented beam-resonator arrangement Fourier-transform microwave spectrometer. *Review of Scientific Instruments* **67**, 4072–4084.

Greaves, JS, Richards AMS, Bains W, Rimmer PB, Sagawa H, Clements DL, Seager S, Petkowski JJ, Sousa-Silva C, Ranjan S, Drabek-Maunder E, Fraser HJ, Cartwright A, Mueller-Wodarg I, Zhan Z, Friberg P, Coulson I, Lee E and Hoge J (2021) Phosphine gas in the cloud decks of Venus. *Nature Astronomy* **5**, 655–664.

Hartwig H and Dreizler H (1996) The microwave spectrum of trans-2,3-dimethyloxirane in torsional excited states. *Zeitschrift für Naturforsch* **51a**, 923–932.

Hartwig H, Kretschmer U and Dreizler H (1995) The ^{33}S nuclear quadrupole hyperfine structure in the rotational Spectrum of ^{32}S, 33S dimethyl disulfide. *Zeitschrift für Naturforsch* **50 a**, 131–136.

Herbst E and van Dishoeck EF (2009) Complex organic interstellar molecules. *Annual Review of Astronomy and Astrophysics* **47**, 427–480.

Imai M, Sakai N, López-Sepulcre A, Higuchi AE, Zhang Y, Oya Y, Watanabe Y, Sakai T, Ceccarelli C, Lefloch B and Yamamoto S (2018) Deuterium fractionation survey toward protostellar sources in the perseus molecular cloud: HNC case. *Astrophysical Journal* **869**, 51.

Jabri A, Van V, Nguyen HVL, Mouhib H, Kwabia Tchana F, Manceron L, Stahl W and Kleiner I (2016) Laboratory microwave, millimeter wave and far-infrared spectra of dimethyl sulfide. *Astronomy & Astrophysics* **589**, A127.

Kojima T (1960) Microwave spectrum of methyl mercaptan. *Journal of the Physical Society of Japan* **15**, 1284–1291.

Kretschmer U (1995) The ^{33}S nuclear quadrupole hyperfine coupling in the rotational spectrum of ^{33}S dimethylsulfoxide. *Zeitschrift für Naturforsch* **50a**, 666–668.

Lederberg, J (1965) Signs of life: criterion-system of exobiology. *Nature* **207**, 9–13.

Loomis RA, Burkhardt AM, Shingledecker CN, Charnley SB, Cordiner MA, Herbst E, Kalenskii S, Lee KLK, Willis ER, Xue C, Remijan AJ, McCarthy MC and McGuire BA (2021) An investigation of spectral line stacking techniques and application to the detection of HC$_{11}$N. *Nature Astronomy* **5**, 88–196.

Lovelock JE (1965) A physical basis for life detection experiments. *Nature* **207**, 568–570.

Majumdar L, Gratier P, Vidal T, Wakelam V, Loison J-C, Hickson K and Caux E (2016) Detection of CH$_3$SH in protostar IRAS 16293-2422. *Monthly Notices of the Royal Astronomical Society* **458**, 1859–11865.

Margulès L, Motiyenko RA, Alekseev EA and Demaison J (2010) Choice of the reduction and of the representation in centrifugal distortion analysis: A case study of dimethylsulfoxide. *Journal of Molecular Spectroscopy* **260**, 23–29.

Maris A, Calabrese C, Favero LB, Evangelisti L, Usabiaga I, Mariotti S, Codella C, Podio L, Balucani N, Ceccarelli C, LeFloch B and Melandri S (2019) Laboratory measurements and astronomical search for thioacetamide. *ACS Earth and Space Chemistry* **3**, 1537–1549.

Melandri S, Evangelisti L, Maris A, Caminati W, Giuliano BM, Feyer V, Prince KC and Coreno M (2010) Rotational and core level spectroscopies as complementary techniques in tautomeric/conformational studies: the case of 2-mercaptopyridine. *Journal of the American Chemical Society* **132**, 10269–10271.

Müller HSP, Thorwirth S, Roth DA and Winnewisser G (2001) The cologne database for molecular spectroscopy, CDMS. *Astronomy & Astrophysics* **370**, L49–L52.

Müller HSP, Schlöder F, Stutzki J and Winnewisser G (2005) The cologne database for molecular spectroscopy, CDMS: a useful tool for astronomers and spectroscopists. *Journal of Molecular Structure* **742**, 215–227.

Müller H, Belloche A, Xu L-H, Lees R, Garrod R, Walters A, Van Wijngaarden J, Lewen F, Schlemmer S and Menten K (2016) Exploring molecular complexity with ALMA (EMoCA): alkanethiols and alkanols in Sagittarius B2(N2). *Astronomy & Astrophysics* **587**, A92.

Neill JL, Steber AL, Muckle MT, Zaleski DP, Lattanzi V, Spezzano S, McCarthy MC, Remijan AJ, Friedel DN, Widicus Weaver SL and Pate BH (2011) Spatial distributions and interstellar reaction processes. *Journal of Physical Chemistry A* **115**, 6472–6480.

Pickett HM (1991) Fitting and prediction of vibration-rotation spectra with spin interactions. *Journal of Molecular Spectroscopy* **148**, 371–377.

Pierce L and Hayashi M (1961) Microwave spectrum, dipole moment, structure, and internal rotation of dimethyl sulfide. *The Journal of Chemical Physics* **35**, 479.

Pilcher CB (2003) Biosignatures of early earths. *Astrobiology* **3**, 471–486.

Sanchez R, Giuliano BM, Melandri S, Favero LB and Caminati W (2007) Gas-phase tautomeric equilibrium of 4-hydroxypyrimidine with its ketonic forms: a free jet millimeterwave spectroscopy study. *Journal of the American Chemical Society* **129**, 6287–6290.

Seager S (2013) Exoplanet habitability. *Science (New York, N.Y.)* **340**, 577–581.

Seager S, Schrenk M and Bains W (2012) An astrophysical view of earth-based metabolic biosignature gases. *Astrobiology* **12**, 61–82.

Segura A, Kasting JF, Meadows V, Cohen M, Scalo J, Crisp D, Butler RAH and Tinetti G (2005) Biosignatures from Earth-like planets around M dwarfs. *Astrobiology* **5**, 706–725.

Shahar A, Driscoll P, Weinberger A and Cody G (2019) What makes a planet habitable? *Science (New York, N.Y.)* **364**, 434–435.

Smeyers YG and Niño A (1987) Character tables and symmetry eigenvectors for two C$_{3v}$ rotor molecular systems. *Journal of Computational Chemistry* **8** 380–388.

Song W, Maris A, Rivilla VM, Fortuna F, Evangelisti L, Lv D, Rodríguez-Almeida L, Jiménez-Serra I, Pintado JM and Melandri S (2022) Microwave- and millimeter-wave spectra of five conformers of cysteamine and their interstellar search. *Astronomy & Astrophysics* **661**, A129.

Typke V (1978) Calculations on the r_z-structure of dimethylsulfoxide. *Zeitschrift für Naturforsch* **33**, 842847.

Uriarte I, Melandri S, Maris A, Calabrese C and Cocinero EJ (2018) Shapes, dynamics, and stability of β-ionone and its two mutants evidenced by high-resolution spectroscopy in the gas phase. *The Journal of Physical Chemistry Letters* **9**, 1497–1502.

Velino B, Melandri S and Caminati W (2004) Internal motions of the rare gas atom in dimethyl ether–krypton. *Journal of Physical Chemistry A* **108**, 4224–4227.

Vigorito A, Calabrese C, Paltanin E, Melandri S and Maris A (2017a) Regarding the torsional flexibility of the dihydrolipoic acid's pharmacophore: 1,3-propanedithiol. *Physical Chemistry Chemical Physics* **19**, 496–502.

Vigorito A, Paoloni L, Calabrese C, Evangelisti E, Favero LB, Melandri S and Maris A (2017b) Structure and dynamics of cyclic amides: the rotational spectrum of 1,3-dimethyl-2-imidazolidinone. *Journal of Molecular Spectroscopy* **342**, 38–44.

Vigorito A, Calabrese C, Melandri S, Caracciolo A, Mariotti S, Giannetti A, Massardi M and Maris A (2018) Millimeter-wave spectroscopy and modeling of 1,2-butanediol: laboratory spectrum in the 59.6–103.6 GHz region and comparison with the ALMA archived observations. *Astronomy & Astrophysics* **619**, A140.

Watson JKG. (1977) *Vibrational Spectra and Structure*, vol. **VI**. Oxford, New York: Elsevier Science Publishers B.V.

Woods R (1966) A general program for the calculation of internal rotation splittings in microwave spectroscopy. *Journal of Molecular Spectroscopy* **21**, 4–24.